

## Maki analysis of spin-polarized tunneling in an oxide ferromagnet

D. C. Worledge and T. H. Geballe

*Department of Applied Physics, Stanford University, Stanford, California 94305*

(Received 22 December 1999)

Spin-polarized tunneling data on  $\text{La}_{2/3}\text{Sr}_{1/3}\text{MnO}_3/\text{SrTiO}_3/\text{Al}$  junctions have been analyzed in terms of numerical solutions to Maki's equations which include the effects of orbital depairing, the Zeeman splitting of the spin states, and spin-orbit scattering. We show that there are two solutions to these equations, and identify the correct solution. High quality fits to the data with these solutions yield a  $\text{La}_{2/3}\text{Sr}_{1/3}\text{MnO}_3$  spin polarization of  $P = +72.0 \pm 1\%$ .

### INTRODUCTION

Recent interest in highly polarized materials<sup>1-3</sup> has seen a rebirth in the measurement of the spin polarization of conducting ferromagnets. Of the three common methods for measuring polarization, spin-polarized photoemission,<sup>1</sup> Andreev reflection,<sup>2</sup> and spin-polarized tunneling,<sup>3</sup> the last technique, pioneered by Meservey and Tedrow,<sup>4</sup> is the most amenable to quantitative analysis, as we show in this paper. In spin-polarized tunneling, a tunnel junction is grown with a thin insulating barrier sandwiched in between a superconducting Al electrode and a counterelectrode composed of the ferromagnetic material under study. A  $dI/dV$  measurement of the junction at low temperatures ( $\sim 0.3$  K) in a field of a few T reveals an asymmetry in the spin split Al density of states (DOS), from which the ferromagnet's polarization can be determined. In order not to quench in such high fields, the Al must be grown very thin ( $\sim 50$  Å) and be carefully aligned with its plane parallel to the field. The low spin-orbit scattering of the Al is crucial—heavier elements with larger scattering cannot be used since the density of states does not split in a field, but simply smears out.

Meservey and Tedrow developed this technique in the 1970s, measuring the spin polarization of Fe, Co, and Ni.<sup>5</sup> Further measurements have been conducted on alloys of the 3d elements,<sup>6</sup> the rare earths,<sup>7</sup> and two Heusler alloys.<sup>3,8</sup> Until now, no spin-polarized tunneling measurements on an oxide ferromagnet have been published. One of the difficulties encountered with oxide ferromagnets [and also the Heusler alloy NiMnSb (Ref. 3)] is the high growth temperature required. This necessitates growing the Al layer last, which in turn means that the native oxide of Al cannot be used as the tunnel barrier. Hence tunnel junctions using ferromagnets which must be grown at high temperatures require an artificial barrier to be deposited—a considerable challenge considering that the barrier must be pinhole free and on the order of 15 Å thick.

In Meservey and Tedrow's original work the spin polarization was extracted from the data using a simple ratio of the conductance peak heights analysis,<sup>4,5</sup> as described below. This analysis is applicable if spin-orbit scattering is not present; Al has small but nonzero spin-orbit scattering. Tedrow and Meservey<sup>5</sup> discussed the possibility of fitting the data to theoretical density of states curves which include the effects of spin-orbit scattering. Engler and Fulde calculated

such curves,<sup>9</sup> and Bruno and Schwartz calculated curves including both spin-orbit scattering and magnetic scattering,<sup>10</sup> but the one published fit to data at that time was poor because orbital depairing was not included.<sup>10</sup> Fulde's review<sup>11</sup> discusses the DOS for either spin-orbit scattering or orbital depairing, but not both. In 1975, Meservey, Tedrow, and Bruno<sup>12</sup> used the theory worked out earlier by Maki,<sup>13</sup> which included both spin-orbit scattering and orbital depairing effects, to fit data from *nonmagnetic* tunnel junctions ( $\text{Ag}/\text{Al}_2\text{O}_3/\text{Al}$ ). The only work which measured spin polarization by fitting data to the full Maki theory was published by Meservey, Paraskevopoulos, and Tedrow in 1980.<sup>7</sup> Unfortunately the  $\text{Gd}/\text{Al}_2\text{O}_3/\text{Al}$  junction used had a very smeared out conductance. With this one exception, Meservey and Tedrow did not fit their data to theoretical curves, but used the simple analysis, sometimes subtracting 6–8% of the polarization to correct for spin-orbit scattering.<sup>4-7</sup> There are two reasons for doing this. First, the full Maki equations are difficult to solve numerically, and second, achieving reasonable fits to the data requires very high quality junctions. In 1985 the first problem was largely solved by Alexander *et al.*,<sup>14</sup> who studied Fermi-liquid effects in thin Al films by tunneling. In the present work we point out that the Maki equations yield multiple solutions, we present a useful method for distinguishing the correct solution, and we use these solutions to fit our data on  $\text{La}_{2/3}\text{Sr}_{1/3}\text{MnO}_3/\text{SrTiO}_3/\text{Al}$  junctions, thus measuring the spin polarization of a ferromagnetic oxide with this technique.

### EXPERIMENT

Thin film planar electrode  $\text{La}_{2/3}\text{Sr}_{1/3}\text{MnO}_3/\text{SrTiO}_3/\text{Al}$  junctions were deposited using laser ablation and sputtering. A  $\text{YBa}_2\text{Cu}_3\text{O}_7$  electrode deposited beneath the  $\text{La}_{2/3}\text{Sr}_{1/3}\text{MnO}_3$  was used to eliminate current crowding.<sup>15</sup> The differential conductance of the junctions was measured in a homemade  $\text{He}^3$  probe, with the  $\text{La}_{2/3}\text{Sr}_{1/3}\text{MnO}_3$  lead negative. Details of the deposition parameters, film characterization, and measurement have been published elsewhere.<sup>16</sup>

### SIMPLE MODEL

In the simple model used to analyze spin polarized tunneling data, which ignores the effects of spin-orbit scattering,

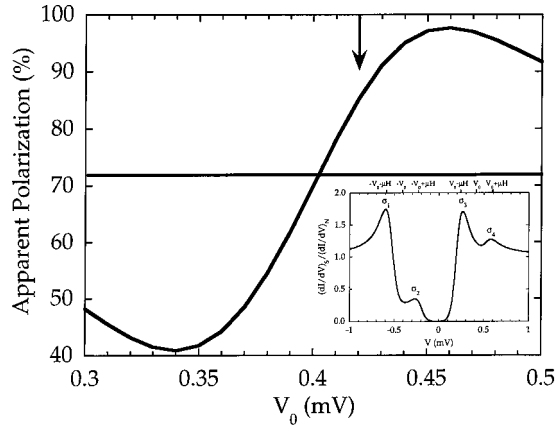


FIG. 1. Dependence of the apparent polarization on the choice of  $V_0$  in the simple ratio of the conductance peak heights method of analysis, which does not take into account spin-orbit scattering. Inset: the conductance curve used to generate Fig. 1, as calculated by the Maki theory for  $T=0.31$  K,  $H=3$  T,  $\Delta=0.39$  mV,  $b=0.05$ , and  $\zeta=0.024$ . The  $\sigma_i$  are evaluated at  $\pm V_0 \pm \mu H/e$ , as noted by the marks at the top of the inset.

$G=dI/dV$  is evaluated at four voltages<sup>4,5</sup> (see inset to Fig. 1):  $\sigma_1=G(-V_0-\mu H/e)$ ,  $\sigma_2=G(-V_0+\mu H/e)$ ,  $\sigma_3=G(V_0-\mu H/e)$ , and  $\sigma_4=G(V_0+\mu H/e)$ . If it is assumed that the DOS is the sum of two identical, spin-split densities of states (i.e., there is no spin-orbit scattering), then it is easy to show that the polarization is given by

$$P = \frac{(\sigma_4 - \sigma_2) - (\sigma_1 - \sigma_3)}{(\sigma_4 - \sigma_2) + (\sigma_1 - \sigma_3)}. \quad (1)$$

The choice of  $V_0$  is arbitrary, and does not affect the result if there is no spin-orbit scattering. In practice, Meservey and Tedrow chose  $V_0$  close to  $\Delta/e$  so that the  $\sigma_i$  were close to the maxima in  $G$ , thus minimizing the dependence on experimental error compounded by a steep slope in  $G$ . However, when spin-orbit scattering is taken into account the apparent polarization extracted with this method depends quite sensitively on the choice of  $V_0$ . Figure 1 shows the apparent polarization, as calculated from Eq. (1), as a function of the choice of  $V_0$ . The inset for Fig. 1 shows the conductance used for this example, as calculated from the exact Maki theory, using typical parameters for our junctions, including an actual polarization of  $P=72\%$ . Also shown are the  $\sigma_i$  used in Eq. (1). Depending on the choice of  $V_0$ , the apparent polarization varies from roughly 41% to over 95%. In particular, the correct polarization, marked by a horizontal line at  $P=72\%$ , lies in the middle of a steeply sloped portion of the curve, making the apparent polarization a sensitive function of  $V_0$ . The vertical arrow at  $V_0=0.42$  mV marks Meservey and Tedrow's choice of  $V_0$  (chosen so as to place the  $\sigma_i$  as close as possible to the maxima in  $G$ ). As seen in this example, this choice of  $V_0$  tends to overestimate the polarization. In practice, Meservey and Tedrow were aware of this problem and so reduced the apparent polarization by a standard 6–8%,<sup>4,6,7</sup> a number which they arrived at from unpublished fits to their data. However, the dependence of this method on the choice of  $V_0$  invites a more accurate method of analysis.

## MAKI THEORY

We have analyzed our results by fitting our data to a theoretical expression for the tunneling conductance. The tunneling conductance is given by

$$dI/dV \propto N_{\uparrow} |M_{\uparrow}|^2 \int_{-\infty}^{\infty} \rho_{\uparrow}(E, H) f'(E+eV) dE + N_{\downarrow} |M_{\downarrow}|^2 \int_{-\infty}^{\infty} \rho_{\downarrow}(E, H) f'(E+eV) dE, \quad (2)$$

where  $N_{\downarrow}$  is the spin down (up) DOS of the ferromagnet at  $E_f$ ,  $M_{\downarrow}$  is the spin down (up) matrix element for transmission,  $\rho_{\downarrow}$  is the spin down (up) superconducting density of states, and  $f'$  is the derivative of the Fermi function with respect to  $V$ . The polarization we measure is given by

$$P = \frac{|M_{\uparrow}|^2 N_{\uparrow} - |M_{\downarrow}|^2 N_{\downarrow}}{|M_{\uparrow}|^2 N_{\uparrow} + |M_{\downarrow}|^2 N_{\downarrow}}. \quad (3)$$

While exact expressions for  $M_{\downarrow}$  are not available (see Mazin<sup>17</sup> for some models), they are essentially constant as a function of energy over the few millivolts of interest here, as are  $N_{\downarrow}$ . Hence we are justified in fitting the data with Al DOS curves, as long as we interpret the measured polarization as being weighted by the spin-dependent transmission probabilities. The Al DOS is given by Maki's theory,<sup>12,13</sup> which includes the effects of orbital depairing, the Zeeman splitting of the spin states, and spin-orbit scattering. In contrast to the investigation of Alexander *et al.*,<sup>14</sup> we do not need to consider Fermi liquid effects<sup>4</sup> as our measurements were done far below the transition temperature where there are few quasiparticles. Maki<sup>12,13</sup> showed that the Al density of states is given by

$$\rho_{\uparrow\downarrow}(E) = \frac{\rho(0)}{2} \operatorname{sgn}(E) \operatorname{Re} \left( \frac{u_{\pm}}{(u_{\pm}^2 - 1)^{1/2}} \right), \quad (4)$$

where  $u_+$  and  $u_-$  are implicitly defined by

$$u_{\pm} = \frac{E \mp \mu H}{\Delta} + \frac{\zeta u_{\pm}}{(1 - u_{\pm}^2)^{1/2}} + b \left( \frac{u_{\mp} - u_{\pm}}{(1 - u_{\mp}^2)^{1/2}} \right). \quad (5)$$

It is important to observe the usual convention that the root with positive real part is chosen. Here  $\rho_{\uparrow\downarrow}$  are again the spin down (up) superconducting density of states, calculated from  $u_+$  ( $u_-$ ),  $\rho(0)$  is the normal density of states,  $E$  is the energy with respect to  $E_f$ ,  $\Delta$  is the energy gap,  $\zeta$  is the orbital depairing parameter, and  $b$  is the spin-orbit scattering parameter. Examination of Eq. (5) suggests that  $u_{\pm}$  take on the BCS values of  $(E \mp \mu H)/\Delta$ , with small lifetime corrections added due to orbital depairing and spin-orbit scattering. In the former case the lifetime is that of a Cooper pair (lifetime for pair breaking), whereas in the latter the lifetime is that of a pure spin eigenstate (lifetime for spin mixing from spin-orbit scattering, which does not break pairs).

Surprisingly, Eq. (5) is difficult to solve for  $u_{\pm}$ . We have discovered that the difficulty lies in the *existence of multiple solutions* to this four-dimensional problem. These multiple solutions have not been noted before, and are discussed below.

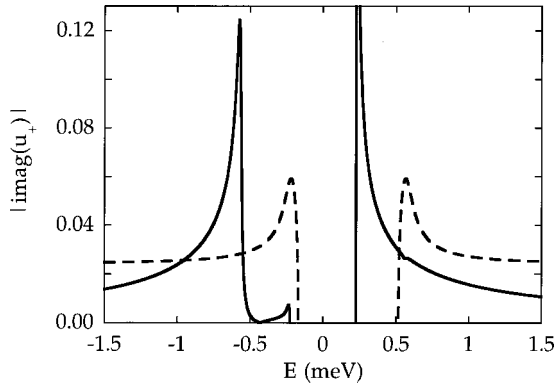


FIG. 2. The magnitude of the imaginary part of  $u_+$  as a function of energy. Both curves were calculated from the Maki theory with  $H=3$  T, and  $\Delta=0.39$  mV. The solid curve has  $b=0.05$  and  $\zeta=0$ , and the dashed curve has  $b=0$  and  $\zeta=0.024$ .

### ANALYSIS OF SOLUTIONS OF MAKI'S EQUATIONS

As a preliminary step we consider Eqs. (5) with either  $b=0$  or  $\zeta=0$ . In these cases straightforward iteration of Eqs. (5) is sufficient, since multiple (nontrivial) solutions only exist when both  $b$  and  $\zeta$  are nonzero. Figure 2 shows the magnitude of the imaginary part of  $u_+$  ( $u_-$  is related by symmetry) for the same parameter choices as in Fig. 1 except with  $b=0$  in one case (dashed line), and  $\zeta=0$  in the other (solid line). The sign of the imaginary part of  $u_+$  is irrelevant, as can be easily deduced from Eq. (4). In Fig. 2 we see in the  $\zeta=0.024$  dashed curve characteristic peaks at  $\pm\Delta + \mu H$  which represent lifetime effects from orbital depairing, and in the  $b=0.05$  solid curve we see peaks at  $\pm\Delta - \mu H$  and  $-\Delta + \mu H$  which represent mixing of the up and down spin states. From Eq. (4) we see that the imaginary part of  $u_+$  is only important when  $|\text{Re}(u_+)|$  is close to or less than one, i.e.,  $|E - \mu H|$  is close to or less than  $\Delta$ . Hence the peak at  $-\Delta - \mu H$  in the  $b=0.05$  curve makes no significant change to  $\rho_{\downarrow}$ . The tall peak at  $\Delta - \mu H$  in the  $b=0.05$  curve gives rise to the extra density of states peak at  $\Delta - \mu H$  in  $\rho_{\downarrow}$ , due to spin mixing<sup>9</sup> (see Fig. 5).

When both  $b$  and  $\zeta$  are nonzero we have discovered that there are two solutions to the Maki equations (in addition to two trivial solutions). In Fig. 3 we show the magnitude of the imaginary part of  $u_+$  as a function of energy for both of these solutions, for the same parameters used in Fig. 1. We see now the presence of peaks at all four energies:  $\pm\Delta - \mu H$ , and  $\pm\Delta + \mu H$ . To help in interpreting these curves, in Fig. 4 we have plotted the same curves as in Fig. 3, and also plotted the magnitude of the sum and difference of the two curves shown in Fig. 2. At large energies (away from the singularities) the sum and difference curves for  $b=0$  and  $\zeta=0$  agree exactly with the two solutions. Hence the two solutions to the Maki equations in Fig. 3 correspond to the orbital depairing and spin-orbit scattering effects adding in phase and out of phase.

At this point it is not clear which of these two solutions is physically significant. To answer this question, we plot in Fig. 5 the DOS curves for spin down electrons, as calculated from Eq. (4), for both solutions. We see that the out of phase solution has a significant amount of extra weight in one of the peaks. The in phase solution does conserve weight,

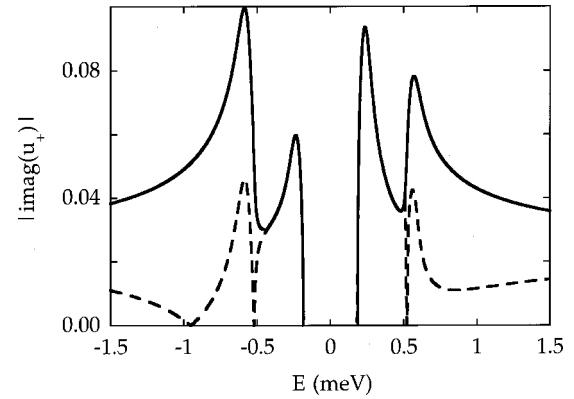


FIG. 3. The magnitude of the imaginary part of  $u_+$  as a function of energy, as calculated from the Maki theory with  $H=3$  T,  $\Delta=0.39$  mV,  $b=0.05$ , and  $\zeta=0.024$ . For these parameter values, there are two solutions to Eq. (5), denoted in phase and out of phase. The in phase solution (solid curve) is the physically meaningful one; the out of phase solution (dashed curve) leads to a density of states which does not conserve weight (see Fig. 5).

whereas the out of phase solution does not. It is not clear what the latter solution corresponds to, physically. In any event, we throw away the nonweight conserving solution, and use the in phase solution.<sup>18</sup>

### NUMERICAL METHOD

Most straightforward applications of the Newton-Raphson method to various rearrangements of Eqs. (5) either do not converge, or converge to only one of the two interesting solutions, regardless of initial conditions. Since one cannot

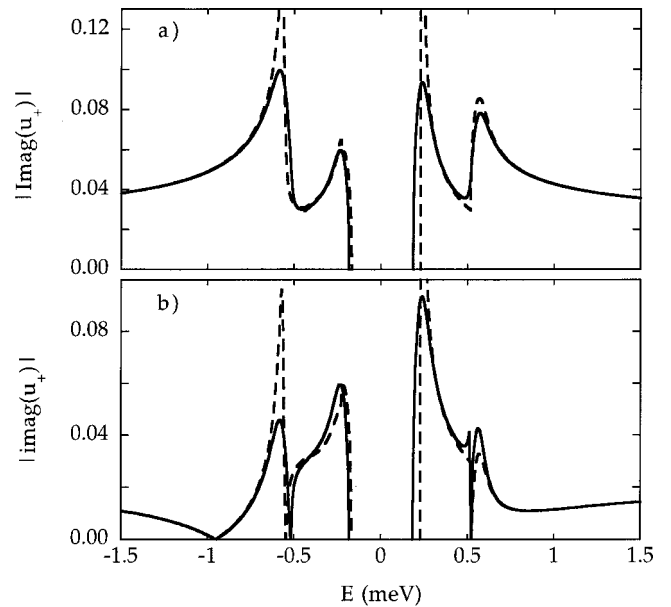


FIG. 4. (a) The solid curve is the in phase solution. The dashed curve is the sum of the curves in Fig. 2. (b) The solid curve is the out of phase solution. The dashed curve is the magnitude of the difference of the curves in Fig. 2. In both (a) and (b), note the agreement between solid and dashed curves at large energies, suggesting that the two solutions to the Maki equations correspond to the orbital depairing and spin-orbit scattering effects adding in and out of phase.

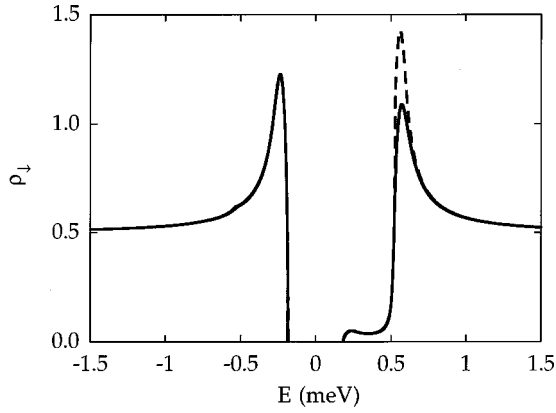


FIG. 5. The spin down density of states, as calculated from Eq. (4). The solid line is from the in phase solution (solid line in Fig. 3) and the dashed line is from the out of phase solution (dashed line in Fig. 3). The out of phase solution does not conserve weight, and so is discarded.

control which solution is converged to, these methods are not general purpose enough to be useful. The most useful method is the one outlined in Ref. 14. Alexander *et al.*<sup>14</sup> generalized Maki's result to include Fermi liquid effects, arriving at four equations in four complex unknowns, which are mathematically equivalent to Eq. (5) when Fermi liquid effects are ignored. The benefit of using these four equations instead of Eq. (5) is that for all choices of parameters, the Newton-Raphson method converges (for  $u_+$ ) to the in phase solution for  $E > 0$  and to the out of phase solution for  $E < 0$ . Since the out of phase solution gives the correct spin down density of states for  $E < 0$  (though not for  $E > 0$ ), the results of this method give the correct spin down density of states for *all* energies. This method also gives the correct spin up density of states.

#### ANALYSIS OF DATA AND DISCUSSION

Armed with this ability to solve the Maki equations, we proceeded to fit our data. The zero temperature solutions of Eq. (4) were thermally smeared using Eq. (2) to give theoretical values of  $(dI/dV)_S/(dI/dV)_N$ . Figure 6 shows the normalized zero field data along with a fit using the measured temperature  $T = 0.31$  K,  $\Delta = 0.39 \pm 0.005$  mV, and  $\zeta = 0.016$ .

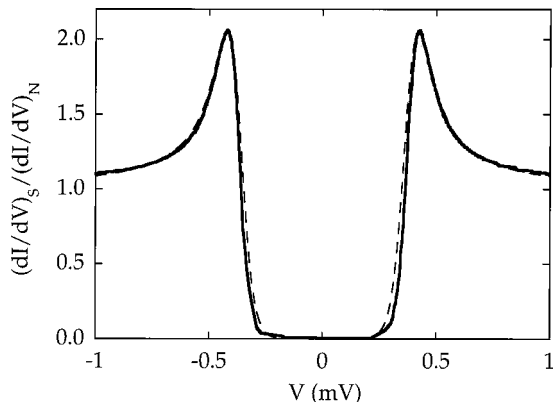


FIG. 6. Normalized data for  $H = 0$  T (solid line), and theoretical fit (dashed line) from Eq. (2) with  $T = 0.31$  K,  $\Delta = 0.39$  mV, and  $\zeta = 0.016$ .

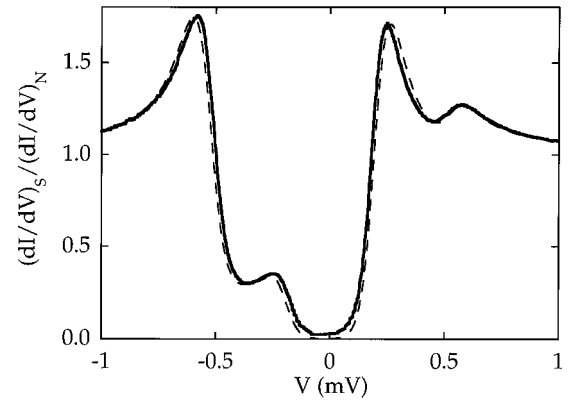


FIG. 7. Normalized data for  $H = 3$  T (solid line), and theoretical fit (dashed line) from Eq. (2) with  $T = 0.31$  K,  $\Delta = 0.39$  mV,  $\zeta = 0.024$ ,  $b = 0.05$ , and  $P = +72.0\%$ .

$= 0.016 \pm 0.0005$ . This finite  $\zeta$  is presumably due to the fringing field from the remnant domain state of the LSMO. We have made over fifty junctions with high quality gaps such as that shown in Fig. 6, which attests to the reproducibility of our technique. All similarly grown junctions have values of  $\Delta$  and  $\zeta$  within a few percent of those quoted here. Figure 7 shows the normalized 3 T data, along with a fit from Eq. (2) with  $\Delta = 0.39$  mV,  $\zeta = 0.024 \pm 0.0005$ ,  $b = 0.05$ , and a polarization of  $P = +72.0 \pm 1\%$ , meaning that  $86 \pm 0.5\%$  of the transport weight comes from spin up electrons, and  $14 \pm 0.5\%$  from spin down. All similarly grown junctions have been fit with values of polarization within a few percent of this. The fit is extremely sensitive to the polarization, and much less sensitive to the values of  $b$  and  $\zeta$ . A different fit with  $P = +70\%$  was too high at  $V = -0.25$  mV, and too low at  $V = +0.25$  mV, showing the sensitivity of the fit to the polarization. We have used the measured temperature  $T = 0.31$  K, the accepted value of  $b = 0.05$  for thin, granular Al,<sup>4</sup> the zero field value for  $\Delta = 0.39$  mV,<sup>19</sup> and only varied  $P$  and  $\zeta$ . Fitting such a complicated curve with only two fitting parameters is good support for Maki's model. The agreement between theory and experiment is significantly better than the limited amount of previously published data.<sup>7,10</sup>

LSMO was theoretically predicted to be highly polarized by Pickett and Singh.<sup>20</sup> Their calculation showed that there were some pockets of minority spins at the Fermi energy, but that these were likely to be localized by disorder, and thus not contribute to the tunneling spin polarization which we measure.

The other two methods referred to in the opening paragraphs, namely spin polarized photoemission and Andreev reflection, have also been used to measure the spin polarization of LSMO. Spin polarized photoemission by Park *et al.*<sup>1</sup> suggested that the surface barrier of cleaned and annealed films of LSMO is 100% spin polarized. It is not clear how this should compare to our tunneling results, since in tunneling the matrix elements favor the highly mobile  $s$ - $d$  hybridized states. Hence, it may be that photoemission and tunneling measure fundamentally different polarizations. Andreev reflection measures yet another type of polarization. The exact form of the polarization is not known, though Mazin<sup>17</sup> has derived several expressions, two of which are valid in the diffusive and ballistic limits. In these limits the spin densities

in Eq. (3) are weighted by powers of the Fermi velocity, instead of by matrix elements. For purposes of comparison between Andreev reflection and tunneling, Mazin has used a particularly simple model to derive an expression for the tunneling polarization. In the limit of an infinitely high delta function barrier he finds the expression for the tunneling polarization is the same as the diffusive Andreev result. However, the Andreev reflection data of Soulen *et al.*<sup>2</sup> on LSMO were taken in the ballistic regime, and so are not directly comparable to our tunneling data. Still, their data give a polarization of 78%, which is in surprisingly good agreement with our result of  $P=72\%$ .

### CONCLUSION

We have demonstrated that the analysis of spin polarized tunneling data by the ratio of the conductance peak heights is susceptible to large errors. Instead we have used numerical

solutions to Maki's equations to unambiguously fit our data. We have shown that there are two solutions to these equations, and have identified the correct solution by appealing to conservation of spectral weight. The correct solutions provided excellent fits to our data on  $\text{La}_{2/3}\text{Sr}_{1/3}\text{MnO}_3/\text{SrTiO}_3/\text{Al}$  junctions. This allowed us to measure the spin polarization of  $\text{La}_{2/3}\text{Sr}_{1/3}\text{MnO}_3$  to be  $P = +72.0 \pm 1\%$ .

### ACKNOWLEDGMENTS

We would like to thank Laurent Mieville and Kookrin Char for many useful discussions, particularly at the early stages of this work. We are also indebted to Blas Cabrera for the basic  $\text{He}^3$  probe and advice on how to finish it. This research was supported by the Air Force Office of Scientific Research, and the National Science Foundation under the MRSEC program.

- 
- <sup>1</sup>J.-H. Park, E. Vescovo, H.-J. Kim, C. Kwon, R. Ramesh, and T. Venkatesan, *Phys. Rev. Lett.* **81**, 1953 (1998).
- <sup>2</sup>R. J. Soulen, Jr., J. M. Byers, M. S. Osofsky, B. Nadgorny, T. Ambrose, S. F. Cheng, P. R. Broussard, C. T. Tanaka, J. Nowak, J. S. Moodera, A. Barry, and J. M. D. Coey, *Science* **282**, 85 (1998). These data are analyzed only at  $V=0$ , without fitting the entire  $dI/dV$  curve, as we do here.
- <sup>3</sup>C. T. Tanaka, J. Nowak, and J. S. Moodera, *J. Appl. Phys.* **86**, 6239 (1999).
- <sup>4</sup>R. Meservey and P. M. Tedrow, *Phys. Rep.* **238**, 173 (1994).
- <sup>5</sup>P. M. Tedrow and R. Meservey, *Phys. Rev. B* **7**, 318 (1973).
- <sup>6</sup>D. Paraskevopoulos, R. Meservey, and P. M. Tedrow, *Phys. Rev. B* **16**, 4907 (1977).
- <sup>7</sup>R. Meservey, D. Paraskevopoulos, and P. M. Tedrow, *Phys. Rev. B* **22**, 1331 (1980).
- <sup>8</sup>P. C. Sullivan and J. S. Rogers, *Solid State Commun.* **45**, 977 (1983).
- <sup>9</sup>H. Engler and P. Fulde, *Z. Phys.* **247**, 1 (1971).
- <sup>10</sup>R. C. Bruno and B. B. Schwartz, *Phys. Rev. B* **8**, 3161 (1973).
- <sup>11</sup>Peter Fulde, *Adv. Phys.* **22**, 667 (1973).
- <sup>12</sup>R. Meservey, P. M. Tedrow, and R. C. Bruno, *Phys. Rev. B* **11**, 4224 (1975).
- <sup>13</sup>K. Maki, *Prog. Theor. Phys.* **32**, 29 (1964).
- <sup>14</sup>J. A. X. Alexander, T. P. Orlando, D. Rainer, and P. M. Tedrow, *Phys. Rev. B* **31**, 5811 (1985). Note the sign error in their Eq. (79); it should be as in Eq. (10) of Ref. 12.
- <sup>15</sup>I. Giaever, in *Tunneling Phenomena in Solids*, edited by E. Burstein and S. Lundqvist (Plenum, New York, 1969); R. J. M. van de Veerdonk, J. Nowak, R. Meservey, J. S. Moodera, and W. J. M. de Jonge, *Appl. Phys. Lett.* **71**, 2839 (1997).
- <sup>16</sup>D. C. Worledge and T. H. Geballe, *Appl. Phys. Lett.* **76**, 900 (2000).
- <sup>17</sup>I. I. Mazin, *Phys. Rev. Lett.* **83**, 1427 (1999).
- <sup>18</sup>We have found a third solution over a limited range of negative energy which gives the same density of states as shown in Fig. 5. Numerical methods cannot rule out the existence of additional solutions.
- <sup>19</sup>The expression (Ref. 12)  $\Delta = \Delta_0 \exp(-\pi\xi/4)$  does not apply here, since we measure  $\Delta_0$  in a remnant field of unknown direction and magnitude, due to the remnant domain structure in the LSMO. When fitting the  $H=3$  T data, for simplicity, we have left  $\Delta$  at the value found in the  $H=0$  T fit. If we allow  $\Delta$  to decrease slightly, as expected, the fit becomes almost perfect.
- <sup>20</sup>W. E. Pickett and D. J. Singh, *J. Magn. Magn. Mater.* **172**, 237 (1997).